International Journal of Advanced Geosciences, 12 (2) (2024) 106-114

International Journal of Advanced Geosciences

Website: www.sciencepubco.com/index.php/IJAG

Research paper

Baseline magnetic susceptibility measurements of rocks in the Precambrian basement terrain of southwestern Nigeria

Cyril C. Okpoli [1] *, Oladunjoye Michael A. [2], Emilio Herrero-Bervera [3]

[1] *Department of Earth Sciences, Adekunle Ajasin University, Akungba-Akoko, Nigeria*
[2] *Department of Geology, University of Ibadan, Ibadan, Nigeria*
[3] *SOEST-HIGP, University of Hawaii at Manoa, USA*
**Corresponding author E-mail: cyril.okpoli@aaua.edu.ng*

Abstract

Petrological, mineralogical and magnetic susceptibility measurements have been studied within the southwestern Nigeria Precambrian basement rocks. Detail geological mapping and core sampling was done for mineralogical characterisation and magnetic susceptibility of the rock samples. Results of the petrographic analyses revealed: quartz, feldspars, hornblende, biotite and opaque (magnetite, ilmenite, maghemite, titanomaghemite) minerals; with minor component of ferromagnesian minerals like hornblende. Quartz, Microcline and Plagioclase alone constitute up to volume fractions 70 % of the rock in the thin section with plagioclase being the most dominant. The magnetic measurements have revealed that the volume susceptibilities K from the investigated samples range from 0.2 to 56,419 X10-6 [SI]. Charrnockites, Granite, biotite granite gneiss, banded gneiss, gneiss, aplite dike, granite, diorite granite gneiss ranges from: 10,059-56,419; 247-12856;0.2-129; 20.4-39.4; 14.1-22,366; 20-8250; 14-30233;4467-6641; and 632-26,921 X 10-6 [SI] respectively. Differential results in the frequency distribution is due varied composition of the paramagnetic (low magnetic susceptibility) and ferromagnetic (high magnetic susceptibility) grains in the rock specimen.

Keywords: *: Southwestern Nigeria; Magnetic Susceptibility; Precambrian Basement; Petrological; Mineralogy.*

1. Introduction

One of the purpose of coring rock samples in the field is to conduct cored rock specimen measurements in the laboratory to decipher rock magnetic susceptibility and paleomagnetic properties of surface and subsurface crustal materials; owed to the variations of their magnetic fields. Most times, rock forming minerals are non-magnetic while some crustal rocks and man-made iron materials have the presence of magnetism. This permits such materials to generate geophysical anomalies. Magnetism has varied areas of applications such as paleomagnetism, environmental magnetism, global plate tectonics, sea floor spreading, archaeological, paleoclimatic and paleogeographic reconstructions (Kearey et al., 2002).

Geomagnetic suites of magnetic susceptibilities of crustal rock materials alongside its petrological studies is crucial in understanding and decrypting its bulk magnetic properties. This integrated studies, unravels rock behaviour and aid the paragenetic sequences that combine in the formation of the rock. The differentiation observed in Earth's magnetic field is caused by geometry, depth, mineralogy, earth's chemistry that played specific roles, resulting to magnetic susceptibilities of the rocks.

Magnetic method measures variation in the Earth's magnetic field caused by changes in the subsurface geological structure or the differences in near-surface rocks' magnetic properties (Telford et al., 1998). Rock samples were cored in the field to conduct laboratory measurements to decipher magnetic susceptibility and paleomagnetic properties on the basis of anomalies in the Earth's magnetic field resulting from the magnetic properties of the underlying rocks. Although most rock-forming minerals are effectively non-magnetic, certain rock types contain sufficient magnetic minerals to produce significant magnetic anomalies. Similarly, man-made ferrous objects also generate magnetic anomalies. Magnetic studies thus have a broad range of applications, from small scale engineering or archaeological studies to detect buried metallic objects, to large-scale surveys carried out to investigate regional geological structure (Kearey et al., 2002).

In this southwestern Nigeria block of Precambrian basement rocks, several geological mapping, mineral exploration and exploitation, geophysical surveys and geochemical characterization have been studied in order to quantify the solid mineral sector of the country (Rahaman et al., 1988; Adetunji et al. 2018). The ground and aeromagnetic magnetic surveys delineates the potential magnetic susceptibilities of various rock units and later interpreted using improved enhancement techniques of fast Fourier transforms (FFT). The magnetic surveys have been the acquisition and processing of the datasets with less emphasis on magneto-mineralogy that create the magnetic susceptibility of rocks. All the previous works in the study area have not addressed subtle paramagnetic sequences that combine to produce the rock fabric (Clark, 1997).

This is the first time cored rock samples from southwestern Nigeria Precambrian basement domain will be measured in the laboratory to unravel the magnetic susceptibilities of various rock specimen with the aim of assessing its magnetic properties as well as the mineralogical composition of the various rock units.

2. Regional geological setting

Neoproterozoic period was the time for reactivation of the southwestern Precambrian basement rocks generally known as Pan-African episodes. Within the Precambrian era there are documentations of older orogenies of isochron ages of 3.57 Ga (Kröner et al., 2001). The study area lies within the west, east and southeast of West African, Saharan and Congo cratons respectively (Fig.1). Caby, 1989 reported that this orogen extends from Hoggar to Brazil to be 4000 km in length and quite a lot of hundreds of Kilometers in width. The 790 Ma and 500 Ma reactivated Trans-Saharan fold belt was caused by the continental deformation of West African craton, Congo Craton and East Saharan block trending north-south direction (Dada 2006; Penaye et al. 2006; Goodenough et al., 2014; Adetunji et al., 2018). This fold belt documents - nappe, granitic and similar tectonic orogeny, medium to high grade metamorphism, (Black and Liégeois 1993). Liégeois et al., 2003 renamed the polycyclic Central Hoggar, Eastern Hoggar and Air Hoggar to the Pharusian belt and LATEA micro continent while the Aïr–Hoggar (Fig. 1) was created by north-south oblique deformation (Liégeois et al., 1994). Around 630 Ma, pseudotachylytes and cataclasites sutured the Neoproterozoic east-dipping subduction observed in Mali and Ifewara-Ilesha shear zones. Caby, 2003 categorised the twenty-three micro blocks aggregates to central and Eastern Hoggar. The Dahomeyide look-like the Air-Hoggar, which is situated at the southern part and extends from eastern border of West African and Congo cratons and consist of numerous blocks (Ajibade and Wright, 1989; Liégeois et al., 1994). Nigerian section of the Dahomeyide is demarcated into Western and Eastern domains, known with preponderance of magmatism during the closure of the prior basin which overlies the weak Archean crust (Ferre et al., 1996; Caby and Boesse 2001). The western and eastern domains is identified with the occurrence of granulite and greenschist-amphibolite facies respectively.

Ferre et al., 2002 studied the northeastern Nigeria Pan –African continental collision which resulted to high grade (HP-HT) metamorphism up to granulite facies, migmatization in supracrustal units which are of the same tectonism with that of eastern Nigeria domain (Onyegocha and Ekwueme 1990). The southwestern Precambrian granitoids is made up of migmatites, schists, Older granites (Archean and Paleoproterozoic isochron ages) and dykes with evidence of 600±150 Ma Pan-African orogenies (Kröner et al., 2001; Okonkwo and Ganev 2012). Neoproterozoic isochron ages are assigned to the Pan-African granitoids and unmetamorphosed dykes which resulted from its tectonometamorphism (Adetunji et al., 2018). Southwestern Nigeria Ifewara-Ilesha, Igarra and Iseyin-Oyan River supracrustals (schists) were deposited and closed in varied proto basins (Rahaman et al., 1988; Ajibade and Wright 1989). On the other hand, Dada (2006); Obaje (2009) subdivided the Precambrian basement rocks into four units. The Pan-African nappe system appears as rejuvenation of older poly-orogenic province as well as tectono-metamorphic events in the whole of Nigerian shield as suggested by numerous authors (Rahaman et al., 1988; Black et al., 1994 and references therein). The grey gneiss consists of biotite and the felsic parts, observed as anastomosing veins of aplite, granite and pegmatite. The schist is predominantly composed of muscovite-biotite with amphibolites outcropping in few places. Charnockite, diorite, granites, associated pegmatites and aplites constitute the Pan-African granitoids. Charnockite occurs as small hills, massive, medium-grained rock. It contains orthopyroxene, clinopyroxene, hornblende, plagioclase, alkali feldspar, magnetite, quartz and zircon (Adetunji et al., 2018). The granite, porphyritic, augen, banded gneiss occur as low lying outcrops and massive hill in some localities.

The Nigerian shield also include low-pressure migmatites and granulites facies with recumbent folds affecting the metasedimentary successions. Progressive charnockitization are recorded in adjacent granitic gneisses and Archean grey gneiss, in which partial melting generated mesoperthite-orthopyroxene bearing leucosomes that fuse to produce intrusive veins. This led to the production of synkinematic granitic, monzonitic, granodioritic, charnockitic massifs. Hot magmas of anhydrous composition of charnockitic affinity, created through a high degree of melting of the lower crust to T_{DM} radiometric ages (Ferre et al., 2002). The gabbroic and syenitic association in the Pan-African rocks demonstrate the magma origin from the enriched mantle coeval with high-temperature metamorphism in the southwestern Nigeria domain (Rahaman et al., 1988).

The study area is situated within the Precambrian basement complex of southwestern Nigeria. The rock samples used for this study are the migmatite-gneiss complex- granites, gneiss, charnockites, aplites, diorites, granodiorites and granite gneiss.

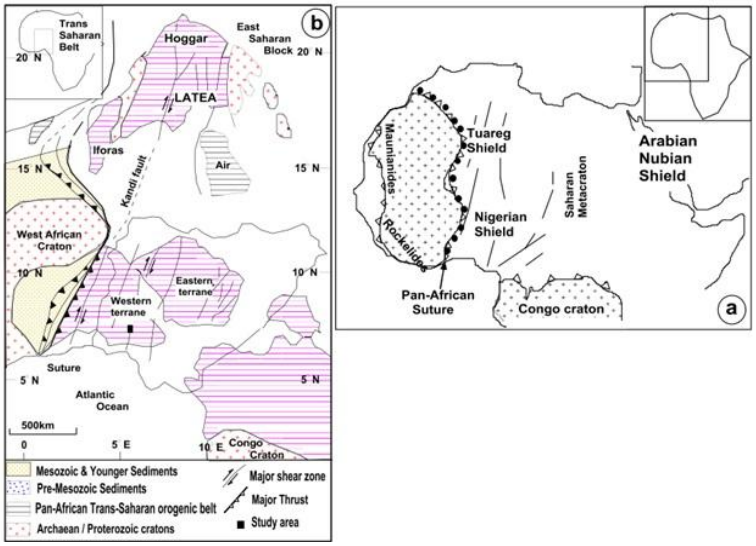

Fig. 1: Regional Geological Map of (A) Pan-African Belt Showing the Tuareg Shield and Nigerian Shield (Modified After Caby, 2003) (B) Trans-Saharan Belt Showing Air-Hoggar and Nigeria Domain (Modified After Ferre Et Al., 2002).

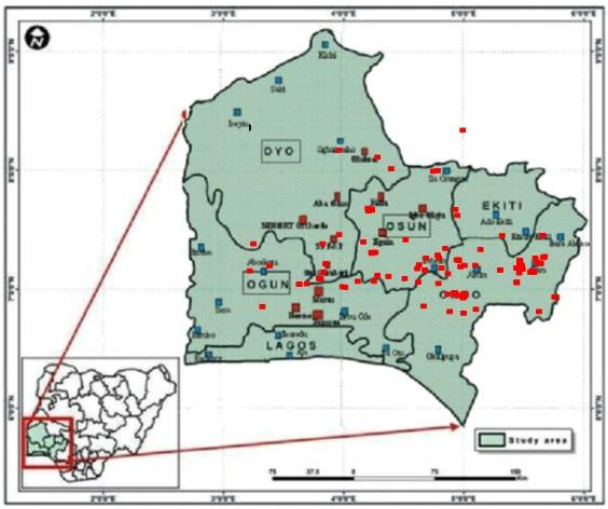

Fig. 2: Location Map Showing the Sampling Points.

2.1. Basic concepts of magnetism and magnetic susceptibility

Presence of normalized moment magnetization M (Am^2), volume normalization M (Am^{-1}) and unit H ($Am^2\ Kg^{-3}$) implies current circuitry and quantum mechanics with electrons and protons that act in response to external fields, resulting to magnetic induction. This process is explained by equation 1:

$$M_I = \chi_b H \quad (1)$$

The non-dimensional scalar bulk magnetic susceptibility parameter is designated as χ_b ; which play the functions of states of temperature and stress, directions of the materials when observed in the fields and its applied field. In real–time practicability, the volume and mass could be normalized or not (Equation 1). Here, the symbol K for the raw measurements is usually utilized.
Some crustal materials do create magnetic fields when there is scarcely any permanent magnetic; resulting to "Spontaneous" magnetic moments. Their results preserve and documents past magnetic fields in crustal rocks and materials. This will yield equation 2, where M, m and l implies dipole magnetic moment, strength and distance respectively:

$$M = ml \quad (2)$$

This phenomenon (magnetic induction) can be used in cross-sectional crustal materials that obtained its magnetism in the direction of the field and loses it when the field is removed. The introduction of J_i with its units Am^{-1} is the intensity of dipole magnetic induction on the material/volume, equation 3 (Kearey et al., 2003).

$$J_I = M/(LA) \quad (3)$$

The intensity of dipole magnetic induction is proportionate to the induced force field of magnetism H and K is magnetic susceptibility as seen in equation 4.

$$J_I = KH \quad (4)$$

In a vacuum the magnetic field; its strength B and magnetizing force H are connected by $B = \mu_0 H$, and μ_0 is not disturbed by any interference, referred as permeability of vacuum ($4\pi \times 10^{-7} Hm^{-1}$). Situations, where we noticed interference, we introduce the strength as $\mu_0 J_i$. Thus, the total magnetic field, B yields equation 5:

$$B = \mu_0 H + \mu_0 J_i \quad (5)$$

Substituting equation (5)

$$B = \mu_0 H + \mu_0 K H = (1 + K)\mu_0 H = \mu_R \mu_0 H \quad (6)$$

Where μ_R implies relative magnetism for other materials (Kearey et al., 2003)

3. Materials and methods

3.1. Sampling

Figure 2 shows the location map and sampling points of the study area. Geological mapping and sampling of rock samples from the Precambrian basement rocks of southwestern Nigeria (Fig. 2); where we cored approximately 235 rocks. The rocks were studied for petrographic, mineralogical and magnetic susceptibility evaluations. The detailed sampling of the rocks involved the Migmatite –gneiss complex of southwestern Nigeria. The number of locations and their cored rock samples are: 5 locations for 37 diorites; 2 locations for 9 granites; 7 locations for 45 charnockites; 2 locations for 10 granite gneiss; another 6 locations for 39 granite having presence of granodiorite; as well as 10 locations for 74 granite having presence of aplite dykes. The magnetic susceptibility measurements were done at the SOEST-

HIGP paleomagnetism laboratory in University of Hawaii at Manoa, USA. We make use of Multifuntional kappabridge (MFK1-FA) for the magnetic susceptibility evaluations.

3.2. Thin sectioning

The following materials were used for the preparation of the thin sections viz: Rock cutting machine, glass plate, carborundum 200, 400, 600 and 800 grits, Canada balsam, aradite, glass slide, cover slips, hot plate, geological hammer, label, methylated spirit, detergent solution, and petrological microscope. These procedures were followed:

1) The samples collected were firstly trimmed with geological hammer,
2) Thereafter, small chips from the samples were then cut and trimmed to about 30×20×4mm using a cutting machine.
3) The chip samples were lapped with carborundum 200, 400 and 600 grits to create a smooth surface,
4) The lapped chips were then mounted on glass slides and put on a hot plate set at 108ºC – 110ºC using aradite as the mounting medium.
5) The mounted chips were then grinded to about 9-6 micrometer thickness on the grinding machine
6) The slides were then further lapped with carborundum 400, 600 and 800grits until a 3 micrometer thickness was reached;
7) Excess adhesive (aradite) was trimmed off from the side of the slides after which it was covered with a cover slip on a hot plate at temperature 105ºC-110ºC. Canada balsam was used as mounting medium
8) Methylated spirit, detergent solution and water was used to clean the slide and were allowed to dry before labeling
9) The slides were then viewed under a petrological microscope.

The average mineral composition was determined under plain polarized light (PPL) and crossed nicols (CN) at a magnification of ×40. Minerals like biotite and hornblende were observed under PPL, under CN, mineral like quartz, plagioclase, microcline and orthoclase were observed. Additional properties like birefringence, form, extinction and twinning were observed under CN.
Average modal analysis was obtained by point counting. At least three views of the slides were observed and the total counts of the minerals were used to divide the total occurrence of a particular mineral. The ratios obtained were converted to the modal composition by multiplying by 100%. It can be calculated as shown below;

Modal Composition = n/N × 100%

Where n = Total counts of a particular minerals from slide views
N = Total points of all the minerals present in the slide views.
The thin section was analysed using petrographical microscope in order to identify the various minerals using their optical properties. The optical properties observed under Crossed Nicol include the Form, Extinction, Twinning and Birefringence; while the optical properties observed under plane polarized light includes Colour, Pleochroism, Cleavage, and Relief.

4. Results and discussions

4.1. Rock mineralogy

Thin section petrography of all the rock units (Tables. 1-7) in the study area shows abundance of Quartz, Microcline and Plagioclase as the major minerals that dominates the rocks samples with other minor components such as hornblende, muscovite and the opaque minerals. Quartz, microcline and Plagioclase minerals were observed to constitute up to volume fractions 70 % of the rock in thin section where plagioclase were seen as the most dominant mineral, and followed secondly by quartz and then microcline being the third most dominant (Plates 1-7).
Furthermore, the quartz mineral contained in the rock samples were colourless under plane polarized light and occurs as subhedral prismatic crystals. Microcline is typified by polysynthetic twinning in two directions (cross-hatched), one according to albite law, and the other according to pericline law whereas plagioclase is distinguished by its polysynthethic twinning according to albite law. Biotite is brown, yellowish brown and reddish brown in thin the section. It is pleochroic occurring as plates and laths and showing elongation along foliation plane. However, muscovite is often seen as the platy brightly coloured minerals while hornblende occur as a ferromagnesian mineral.
The classification of the three rock types in the QAP diagram suggested grey gneiss, which is substantially different from the granitic and granite gneissic rock petrologically, it further revealed that the granite gneiss and the granitic rock were monzo-granitic in composition while grey gneiss being granodioritic in composition.

Table 1: Granite (Slide A)

Mineral	Quartz	Plagioclase	Microcline	Biotite	Hornblende	Opaque	Muscovite	Total
(%) Modal Composition	24.1	32.1	22.4	16.8	2.5	0.6		100%

Table 2: Granite Gneiss (Slide B)

Mineral	Quartz	Plagioclase	Microcline	Biotite	Hornblende	Opaque	Muscovite	Total
Modal Composition (%)	27.6	32.1	24.1	13	3.5	0.7		100%

Table 3: Grey Gneiss (Slide C)

Mineral	Quartz	Plagioclase	Microcline	Biotite	Hornblende	Opaque	Muscovite	Total
Modal Composition (%)	26	30.3	20.1	17.8	3.2	0.6	1	100%

Table 4: Banded Gneiss (Slide D)

Mineral	Quartz	Plagioclase	Microcline	Biotite	Hornblende	Opaque	Muscovite	Total
Modal Composition (%)	28.2	31.2	23	9.5	4.2	0.8	3.1	100%

Table 5: Granite Gneiss (Slide E)

Mineral	Quartz	Plagioclase	Microcline	Biotite	Hornblende	Opaque	Muscovite	Total
Modal Composition (%)	30.5	33.9	28.1	2.2		0.3	5	100%

Table 6: Granite 2 (Slide F)

Mineral	Quartz	Plagioclase	Microcline	Biotite	Hornblende	Opaque	Muscovite	Total
Modal Composition (%)	24.1	32	20.3	15	5.2	0.7	2.7	100%

Table 7: Grey Gneiss (Slide G)

Mineral	Quartz	Plagioclase	Microcline	Biotite	Hornblende	Opaque	Muscovite	Total
Modal Composition (%)	26.2	30.2	24.2	10.9	2.5	0.5	5.5	100%

Table 8: Average Modal Analysis of the Following Rock Samples

SAMPLE NO	QUARTZ	MICROCLINE	PLAGIOCLASE	BIOTITE	HORNBLENDE	MUSCOVITE	OPAQUE	TOTAL %
Granite	27.6	24.1	32.1	13	3.5	-	0.7	100
Granitegneiss	24.4	22.4	32.1	16.8	2.5	-	0.6	100
Greygneiss	26	20.1	30.3	17.8	3.2	1	0.6	100
Bandedgneiss	28.2	23	31.2	9.5	4.2	3.1	0.8	100
Granitegneiss	30.5	28.1	33.9	2.2	--	5	0.3	100
Granite	24.1	20.3	32	15	5.2	2.7	0.7	100
Greygneiss	26.2	24.2	30.2	10.9	2.5	5.5	0.5	100

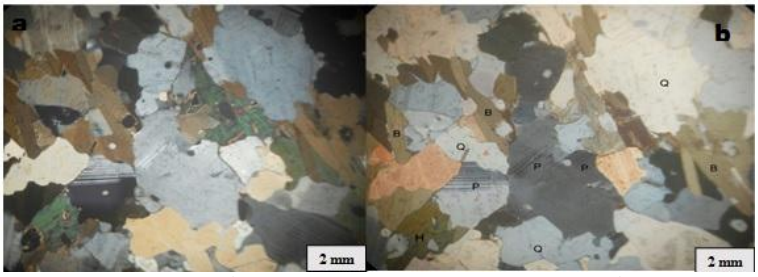

Plate 1: (A) Photomicrograph of Slide A Under PPL, (B) Photomicrograph of Slide A Under XPL.

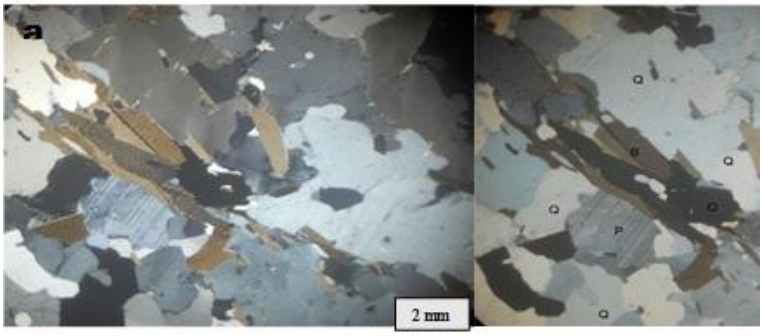

Plate 2: (A) Photomicrograph of Slide B Under PPL, (B) Photomicrograph of Slide B Under XPL.

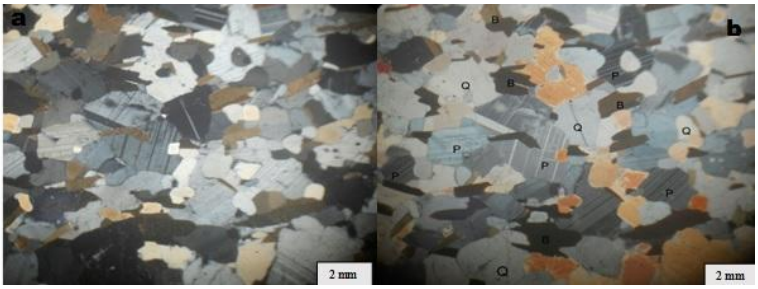

Plate 3: (A) Photomicrograph of Slide C Under PPL, (B) Photomicrograph of Slide C Under XPL.

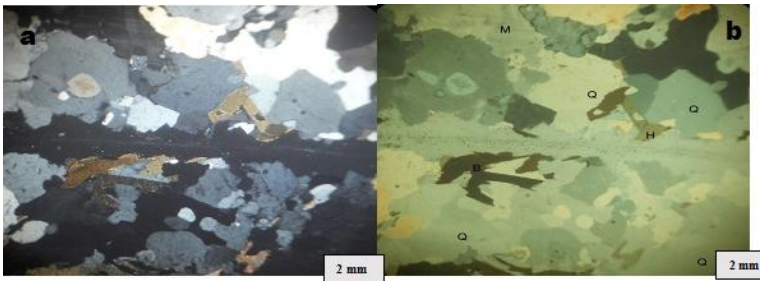

Plate 4: (A) Photomicrograph of Slide D Under PPL, (B) Photomicrograph of Slide D Under XPL.

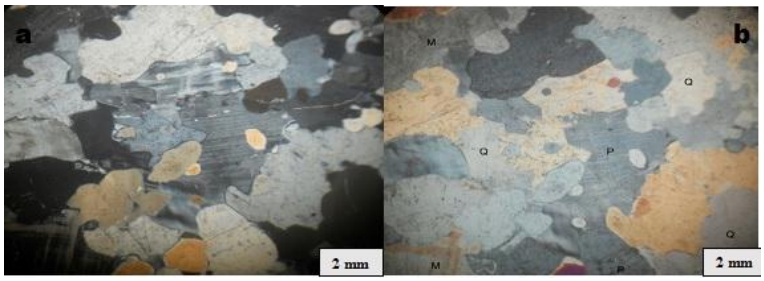

Plate 5: (A) Photomicrograph of Slide E Under PPL, (B) Photomicrograph of Slide E Under XPL.

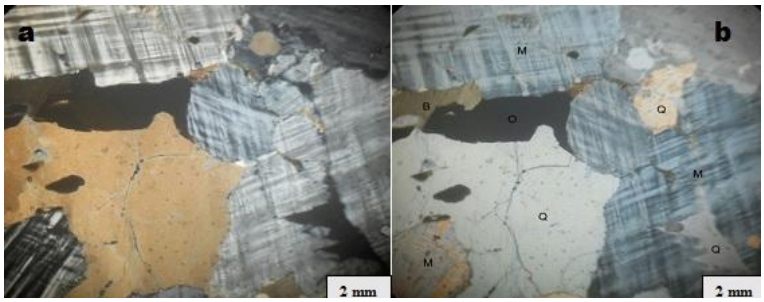

Plate 6: (A) Photomicrograph of Slide F Under PPL, (B) Photomicrograph of Slide F Under XPL.

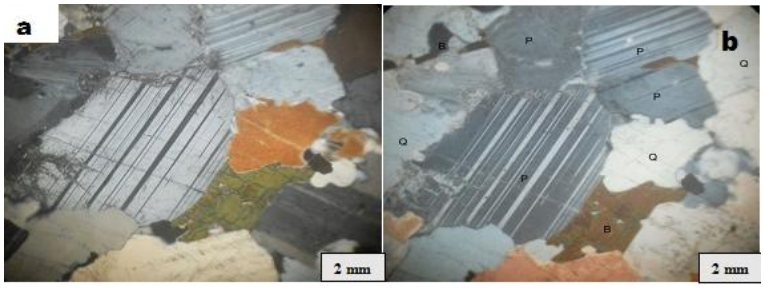

Plate 7: (A) Photomicrograph of Slide G Under PPL(B) Photomicrograph of Slide G Under XPL.

4.2. Rock magnetic susceptibility

Charnockitic and Granitic rocks are significantly high. Their magnetic susceptibility values ranges between 1400 and 30,000 X 10^{-6} [SI] excluding some locations having relative low magnetic susceptibility due to the rock fractured networks. Diorites has higher mean magnetic susceptibility compared to granites and gneiss; however, gneisses with coarser grains witnessed maximum values in some locations. One of the granite rocks measured maximum magnetic susceptibility value of 30,233 X 10^{-6} [SI] as obtained in (73), while other locations documents relatively high magnetic susceptibility values. The mean magnetic susceptibility of charnockitic rocks is relatively high ranging between (6272–17,910 X 10^{-6} [SI]). Most magnetic susceptibility of gneissic rocks is low compared to one location that recorded 9324 X 10^{-6} [SI] as maximum. Locations 44 and 48 in dioritic rocks documented magnetic susceptibility greater than 18,300 X 10^{-6} [SI]), although is not > 4190 X 10^{-6} [SI] in the granitic rock. Aplitic dykes recorded mean susceptibility as relatively low as (<900 X 10^{-6} [SI]) apart from three locations where it was observed in granitic rocks having 1496 and 8250 X 10^{-6} [SI] measurements. Nonetheless, most of the sampled dykes recorded lower magnetic susceptibility than the widely distributed granitic and dioritic rocks.

Aplitic dykes mean magnetic susceptibility is largely weak, apart from two locations in granitic rock (where it is relatively higher). Some aplite dyke (Figure 4b) of the Granitic rock, maintain the same magnetic axes directions with their host rock (granite). In some locations we have magnetic intensity value approximately up to 1.52 when compared to 1.04 observed in the granitic host rock. This was not documented in several Aplitic dykes observed in the study area that found itself concordant to the host rocks. Some dioritic dyke in the granite rock depicts differing higher magnetic susceptibility (4468 X10^{-6} [SI]) than the granitic host-rock (1646 X 10^{-6} [SI]).

Figure 6b depicts the mean magnetic susceptibility of values comparatively higher than Figure 3b; diorite (11,141 X 10^{-6} [SI]) greater than gneiss (8456 X 10^{-6} [SI]) (Fig. 6b). Gneiss witnessed differential mean magnetic susceptibility in both locations, the highest values were recorded in locations 5 and 6 of the Gneissic rock (>29,100 X 10^{-6} [SI]). The average of the mean magnetic susceptibility values, suggested a drop in susceptibility in some locations, due to the fractured networks. Location 6 has the highest magnetic intensity of 1.30 while the highest value documented 1.50 in the aplitic dyke observed in location 21 of granite rock (PO = 1.23); the aplite and granite tectonized location. Granite rocks have average P0 values amid 1.08 and 1.16, which does not differ considerably from that in the Biotite granite gneiss locations of PO values between 1.05 and 1.12.

Figure 5b illustrate the frequency distribution of the mean magnetic susceptibility in the granitic rock that recorded 9080 X 10^{-6} [SI] reaching more than 30,000 X 10^{-6} [SI] in some locations higher than in the gneiss (Fig. 6b) where the mean magnetic susceptibility values have an average of 3300 X 10^{-6} SI). The area, observed drop in the mean magnetic susceptibility values, that is <4191 X 10^{-6} [SI]. Some locations toward the northwest-southeast fault line rock networks, witnessed drop in the susceptibility values. Thus, the low PO values, ranges from 1.02 to 1.06. On the other side, dioritic rocks have relatively high mean susceptibility values (15,460–18,238 X 10^{-6} [SI]) in all the sampled locations. Their P0 values ranges between 1.03 and 1.06, which are slightly higher than others.

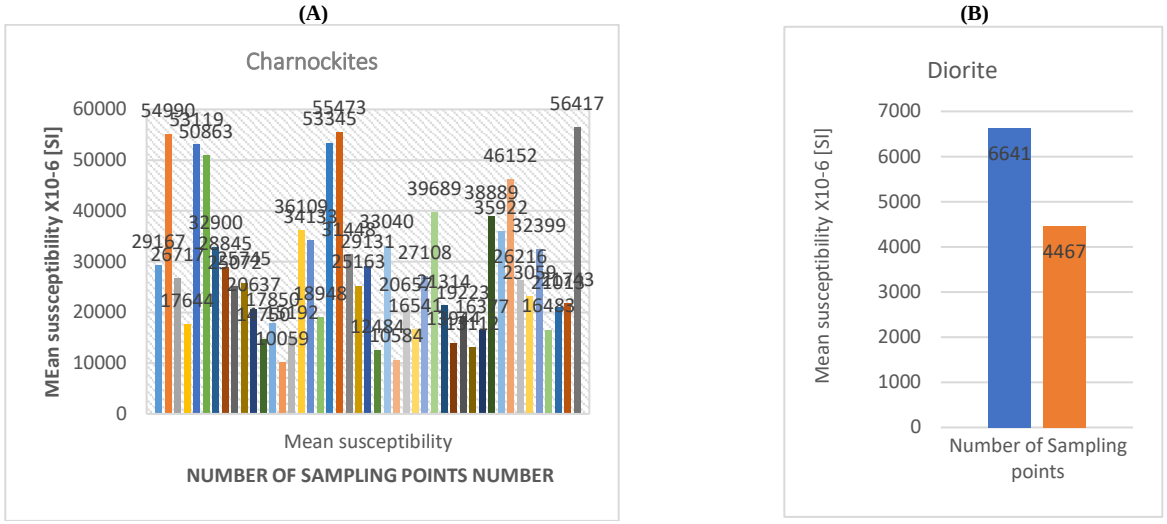

Fig. 3: (A)Frequency Distribution Plot for Charnockites and (B) Diorite.

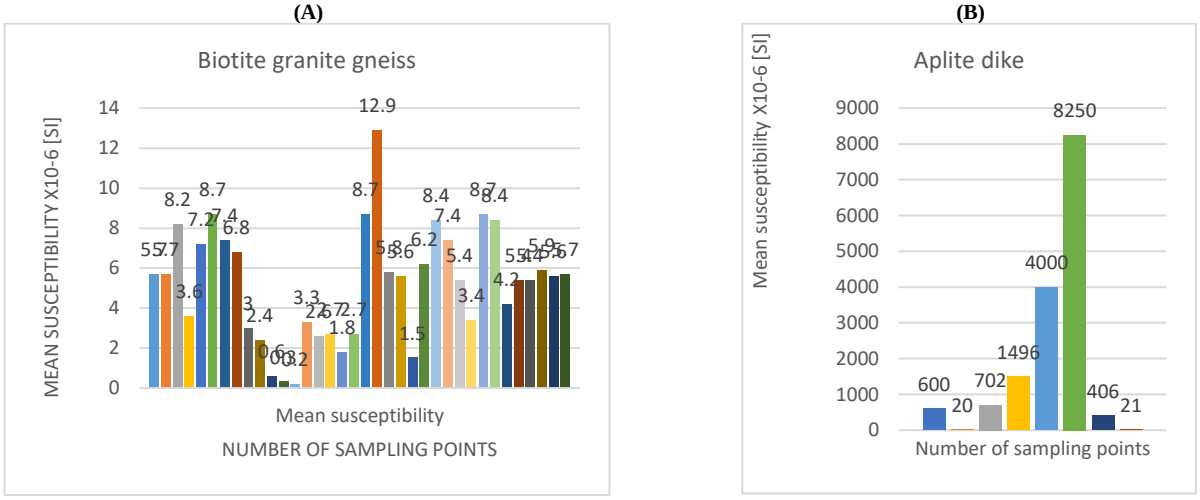

Fig. 4: (A)Frequency Distribution Plot for Biotite Granite Gneiss and (B) Aplite Dike.

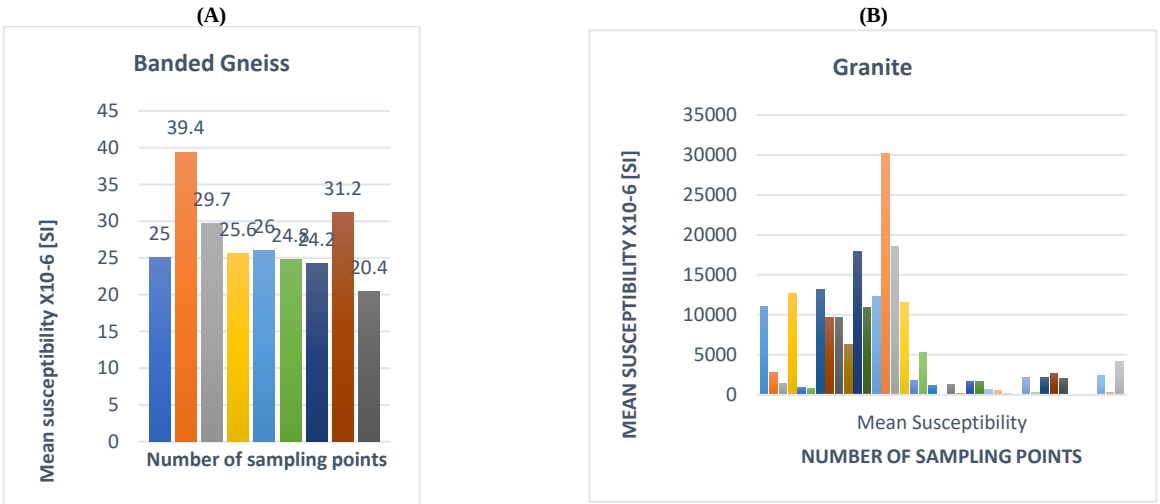

Fig. 5: (A)Frequency Distribution Plot for Banded Gneiss and (B) Granite.

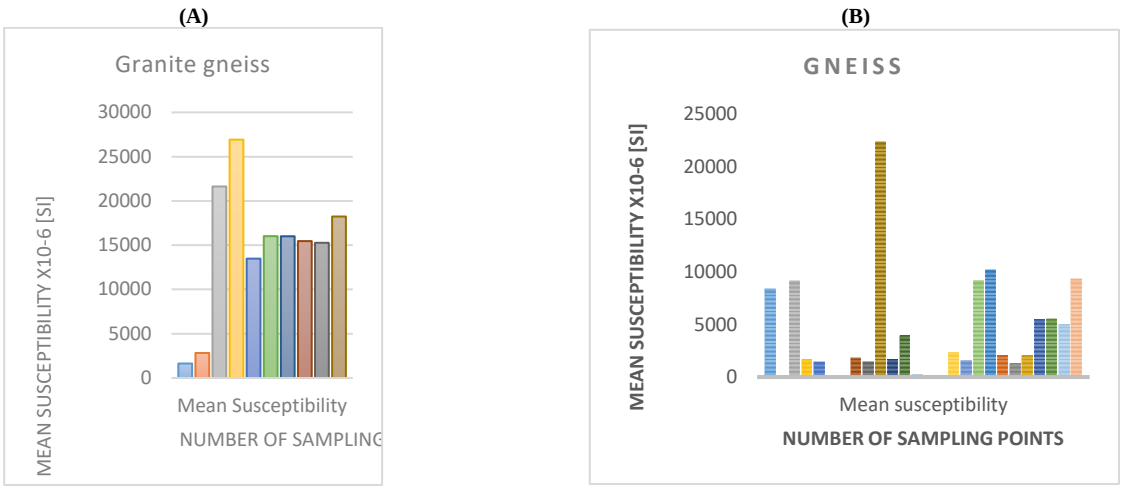

Fig. 6: (A) Frequency Distribution Plot for Granite Gneiss and (B) Gneiss.

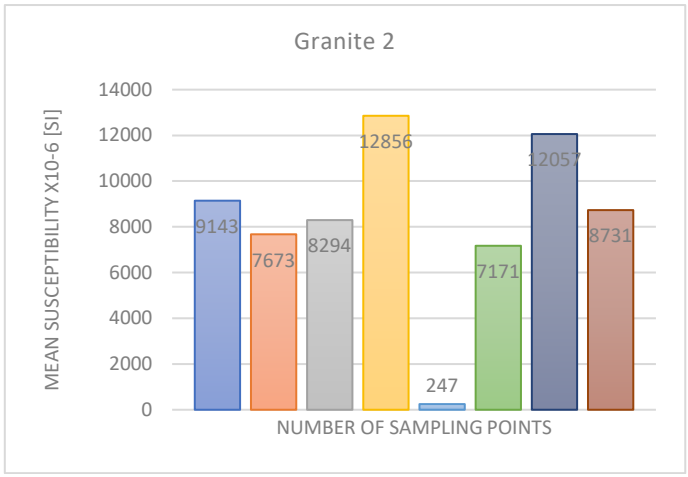

Fig. 7: (A)Frequency Distribution Plot for Granite 2.

5. Discussions

Ferromagnetic, paramagnetic and diamagnetic grains are generally present in rocks. The diamagnetic contribution originates from feldspar and quartz while magnetites, titanomagnetite, maghemite etc. are ferromagnetic. The quartz has a fundamental negative magnetic susceptibility of 13.4 X 10^{-6} [SI] (Hrouda, 1986) while feldspar has 2.76 X 10^{-6} [SI] (Borradaile et al., 1987). Their contributions are usually insignificant in mineralogical, geochemical characterization and global tectonics (Borradaile and Henry, 1997). Thus, the impacts of magnetism to magnetic susceptibility in southwestern Precambrian rocks are due to the paramagnetic minerals while biotite and plagioclase have greater percentage of abundance in the region. Magnetite, maghemite and titanomagnetite and ilmenite were observed in trace ferromagnesian minerals. Most of the samples have predominance of maghemite in the southwestern terrain due to several tectono-metamorphic events. Thus, the various rocks samples studied and their magnetic susceptibilities are depicted with frequency histograms (Figs. 3-7). The frequency distribution of granites, charnockites, aplite, gneiss, diorites has differential modal, which suggested combination of three factors that are indistinguishable: mineral content differentiation within an outcrop, random error of measurements and the cross-cutting rocks and dykes observed in a typical rock unit. Ajakaiye (1989) described types disparity and its implications owed to the inhomogeneity of the Precambrian basement complex; which is caused by several orogenic activity of the past.

6. Conclusion

Petrographic analysis of the study area revealed that quartz, feldspars, hornblende, biotite and opaque (magnetite, ilmenite, maghemite, titanomaghemite) minerals constitute the major minerals identified in thin section of the rock units, with minor component of ferromagnesian minerals like hornblende. Quartz, Microcline and Plagioclase alone constitute up to volume fractions 70 % of the rock in the thin section with plagioclase being the most dominant.

The geochemical assessment showed that SiO_2 (silica) is by far the most abundant mineral in all the rock types with the highest percentage present in the granitic rock and lowest in the granite gneissic rock. Hence, based on silica content, the granitic rocks are more silicic or acidic than the grey gneisses, while granite gneiss being the least siliceous.

The studied rock types for magnetic susceptibility in the southwestern Nigeria are: Granite, charnockite, biotite granite gneiss, diorite, aplite dike, banded gneiss and gneiss. The magnetic measurements suggested that the volume susceptibilities K from the rock samples studied ranges from 0.2 to 56,419 X 10^{-6} (SI). Charrnockites, Granite, biotite granite gneiss, banded gneiss, gneiss, aplite dike, granite, diorite granite gneiss ranges from: 10,059-56,419; 247-12856;0.2-129; 20.4-39.4; 14.1-22,366; 20-8250; 14-30233;4467-6641; and 632-26,921 X 10^{-6} (SI) respectively. The result revealed that the magnetic susceptibility recorded in the study area is predominantly controlled by paramagnetic mineral and some samples being controlled by ferromagnetic grains.

Acknowledgements

The First author is grateful to SOEST-HIGP, University of Hawaii at Manoa, USA for his PhD internship. The authors appreciate the positive reviews of the anonymous reviewers.

References

[1] Adetunji, A., Olarewaju, V.O., Ocan, O.O., Macheva L., and Ganev V.Y., 2018, Geochemistry and U-Pb zircon geochronology of Iwo quartz potassic syenite, southwestern Nigeria: Constraints on petrogenesis, timing of deformation and terrane amalgamation, Precambrian Research 307: 125–136. https://doi.org/10.1016/j.precamres.2018.01.015.
[2] Ajaikaiye, D.E., 1989, Densities of Rocks within the Nigerian Younger granite. In Kogbe, C. A. (Ed.): Geology of Nigeria. Elizabeth Publishers.
[3] Ajibade, A.C., and Wright, J.B., 1989, The Togo-Benin-Nigeria shield: evidence of crustal aggregation in the Pan African belt. Tectonophysics 65:125-129. https://doi.org/10.1016/0040-1951(89)90041-3.
[4] Black, R., Latouche, L., Liegeois, J., Caby, R., and Bertrand, J.M., 1994, Pan-African displaced terranes in the Tuareg shield (central Sahara). Geology 22 (7): 641-644. https://doi.org/10.1130/0091-7613(1994)022<0641:PADTIT>2.3.CO;2.
[5] Black, R., and Liégeois, J.P., 1993, Cratons, mobile belts, alkaline rocks and continental lithospheric mantle: The Pan-African testimony. Journal of Geological Society London 150, 89–98. https://doi.org/10.1144/gsjgs.150.1.0088.
[6] Borradaile, G.J., and Henry, B., 1997, Tectonic applications of magnetic susceptibility and its anisotropy, Earth Science Reviews 42: 49–93. https://doi.org/10.1016/S0012-8252(96)00044-X.
[7] Borradaile, G.J., Keeler, W., Alford, C., and Sarvas, P., 1987, Anisotropy of magnetic Susceptibility of some metamorphic minerals, Physics of Earth Planetary Interiors 48:161–166. https://doi.org/10.1016/0031-9201(87)90119-1.
[8] Caby, R., 1989, Precambrian terranes of Benin-Nigeria and northeast Brazil and the late Proterozoic South Atlantic fit, Geology Society of America Special Paper 230: 145-645. https://doi.org/10.1130/SPE230-p145.
[9] Caby, R.,and Boesse, J.M., 2001, Pan-African Nappe System in South-West Nigeria: 'Ife lle-llesha Schist Belt, Journal of African Earth Science 33 (2): 21 I-225. https://doi.org/10.1016/S0899-5362(01)80060-9.
[10] Caby, R., 2003. Terrane assembly and geodynamic evolution of central–western Hoggar: a synthesis, Journal of African Earth Science 37: 133–159. https://doi.org/10.1016/j.jafrearsci.2003.05.003.
[11] Clark, D.A., 1997. Magnetic petrophysics and magnetic petrography: aids to geological interpretation of magnetic surveys. AGSO Journal of Australian Geology and Geophysics 17: 83–103.
[12] Dada, S.S., 2006, Proterozoic evolution of Nigeria. In: Oshin, O. (Ed.), The Basement Complex of Nigeria and its Mineral Resources (A Tribute to Prof. M. A. O. Rahaman). Akin Jinad & Co., Ibadan, pp. 29–44.
[13] Ferre, E., Gleizes, G., and Caby, R., 2002, Obliquely convergent tectonics and granite emplacement in the Trans-Saharan belts of Eastern Nigeria: a synthesis. Precambrian Research 114: 199-219. https://doi.org/10.1016/S0301-9268(01)00226-1.
[14] Ferre, E., De´le´ris J., Bouchez, J.L., Lar, A.U., and Peucat, J.J., 1996, The Pan-African reactivation of contrasted Eburnean and Archaean provinces in Nigeria: structural and isotopic data. Journal of the Geological Society, London 153: 719–728. https://doi.org/10.1144/gsjgs.153.5.0719.
[15] Goodenough, K.M., Lusty, P.A.J., Roberts, N.M.W., Key, R.M., and Garba, A., 2014, Post collisional Pan-African granitoids and rare metal pegmatites in western Nigeria: age, petrogenesis and the pegmatite conundrum. Lithos 200–201: 22–34 https://doi.org/10.1016/j.lithos.2014.04.006.
[16] Hrouda, F., 1986, The effect of quartz on the magnetic anisotropy of quartzite, Stud. Geophys. Geod. 30: 39–45. https://doi.org/10.1007/BF01630853.
[17] Kearey, P., Brooks, M., and Hill, I., 2002, An Introduction to Geophysical Exploration. 3rded. Blackwell Publishing. 255p.
[18] Kearey, P., Nabighian, M.N., Grauch, J.S., Hansen, R.O., LaFehr, T.R., Li, Y., Peirce, and Phillips, J.W., 2003, The historical development of the magnetic method in exploration Geophysics, 70: 33ND-61ND. https://doi.org/10.1190/1.2133784.
[19] Kröner, A., Ekwueme, B.N.,and Pidgeon, R.T., 2001, The Oldest Rocks in West Africa: SHRIMP Zircon Age for Early Archean Migmatitic Orthogneiss at Kaduna, Northern Nigeria. Journal of Geology 109: 399–406. https://doi.org/10.1086/319979.
[20] Liégeois, J.P., Black, R., Navez, A.J., and Latouche, L., 1994, Early and late Pan-African orogenies in the Aïr assembly of terranes (Tuareg shield, Niger). Precambrian Research 67: 59-88. https://doi.org/10.1016/0301-9268(94)90005-1.
[21] Liégeois, J.P., Latouche, L., Boughrara, M., Navez, J.,and Guiraud, M., 2003, The LATEA metacraton (Central Hoggar, Tuareg shield, Algeria): behaviour of an old passive margin during the Pan-African orogeny. Journal of African Earth Science 37:161–190. https://doi.org/10.1016/j.jafrearsci.2003.05.004.
[22] Obaje, N.G., 2009, Geology and Mineral Resources of Nigeria, Lecture Notes in Earth Sciences Springer Verlag, Berlin,p. 221 https://doi.org/10.1007/978-3-540-92685-6.
[23] Okonkwo, C.T., and Ganev, V.Y., 2012, U-Pb zircon geochronology of the Jebba granitic gneiss and its implications for the Paleoproterozoic evolution of Jebba area, southwestern Nigeria. International Journal of Geosciences 3:1065–1073. https://doi.org/10.4236/ijg.2012.35107.
[24] Onyeagocha, A.C., and Ekwueme, B.N., 1990, Temperature pressure distribution patterns in metamorphosed rocks of the Nigerian Basement Complex a preliminary analysis. https://doi.org/10.1016/0899-5362(90)90079-T.
[25] Journal African Earth Sciences 11: 83-93.
[26] Penaye, J., Kröner, A., Toteu, S.F., Van Schmus, W.R., and Doumnang, J.C., 2006, Evolution of the Mayo Kebbi region as revealed by zircon dating: An early (ca. 740 Ma) Pan African magmatic arc in southwestern Chad. Journal of African Earth Science 44: 530–542. https://doi.org/10.1016/j.jafrearsci.2005.11.018.
[27] Rahaman, M.A.O., Ajayi, T.R., Oshin, l.O., and Asubiojo E.O.L., 1988, Trace clement geochemistry and geotectonic setting of lfewara-llcsha Schist Belt. Precambrian Geology of Nigeria, L 241-256.
[28] Telford, W.M., Geldart, L.P., and Sheriff, R.E., 1998, Applied Geophysics, (2nd Ed), Cambridge University Press, USA, pp. 113 – 114.